

# Quantitative Detection of Bioassays with a Low-Cost Image-Sensor Array for Integrated Microsystems\*\*

Daynene M. Vykoukal, Gregory P. Stone, Peter R. C. Gascoyne, Eckhard U. Alt, and Jody Vykoukal\*

A considerable global need exists for simple, portable, inexpensive, and integrated assay and diagnostic approaches that are appropriate for use in minimal-infrastructure, resource-poor settings, such as those found in the developing world, as well as in resource-limited environments, such as those encountered by emergency first responders, primary-care physicians, patients at home, forensic investigators, and military field personnel.<sup>[1–3]</sup> Continuing advances in microfluidics have enabled the demonstration of prototype lab-on-a-chip devices that offer to help answer this challenge and improve access to chemical and biological sample analysis by paving the way for the introduction of low-cost, portable point-of-need assay systems. Although such systems would have immediate applications in many fields, there are at present relatively few commercially available examples of the technology.<sup>[4,5]</sup>

In clinical and industrial laboratory analyses, the most widely used and generally accepted methods to quantify particulate chemical or biochemical analytes employ optical detection approaches based on absorbance, fluorescence, or luminescence. Although lab-on-a-chip implementations of optical methods have been demonstrated, detection is typically carried out off-chip by using conventional microscope optics and digital-camera systems or custom and relatively expensive chip-scale optoelectronics.<sup>[6,7]</sup> The translation of these established methods into truly portable total-analysis microsystems has been hindered in part by a lack of reasonably priced, sensitive, and compact optical detectors that can be interfaced readily with microfluidic sample handling.<sup>[4,7]</sup> In response to this limitation, we demonstrate the feasibility of applying an inexpensive, readily available complementary metal–oxide–semiconductor (CMOS) image

sensor, originally intended for use in mass-market digital-camera applications, for integrated optical detection in a variety of microfluidic systems. Specifically, we report the direct integration of this chip-scale sensor with our digital fluid-handling system to track nanoliter-volume reagent droplets by contact imaging. We also show the more general application of the sensor as a quantitative photometer for the integrated optical detection of colorimetric and bioluminescence assays implemented in various lab-on-a-chip architectures.

Point-of-need assay platforms will complement, rather than supplant, existing laboratory-based analysis methods and hardware that form the foundation of clinical diagnostics and academic research. Indeed, within the realm of analytical (and in particular, diagnostic) technology and instrumentation, the development of inexpensive point-of-need assays is a rather specific, but not inconsequential endeavor. Over 95 % of deaths due to major infectious diseases occur in developing countries. Although these diseases are largely treatable with drug therapy, the lack of available, infrastructure-appropriate diagnostic assays means that healthcare workers in these settings are unable to identify who is, or—just as critically—is not, in need of treatment.<sup>[2,3]</sup> Simple, portable, inexpensive assay systems are also of value in natural-disaster and other emergency situations that arise indiscriminately in all countries.<sup>[8]</sup>

Technology and instrumentation for performing chemical and biochemical analyses have, thus far, typically been advanced to meet the demands of comparatively well-funded laboratories. State-of-the-art assay systems employing flow-injection analysis (FIA),<sup>[9,10]</sup> automated microplate processors and readers, or other mechanized sample-handling technologies,<sup>[11,12]</sup> provide impressive capabilities for continuous or parallel processing and the assaying of hundreds or thousands of samples per hour (sample preparation and readout times combined can average well under one second per sample). Thus, they are especially useful in centralized laboratories where high-throughput is essential. Whereas such systems are currently the mainstay of clinical diagnostics, drug discovery, and many research laboratories (and will probably remain so for the foreseeable future), the primary target of lab-on-a-chip assay approaches is to provide “sample in, answer out” assay capabilities by integrating sample handling and processing steps into a closed microfluidic, often single-use, architecture that is more ideally suited for localized assay applications.

It is probable that many analyses will remain the province of dedicated centralized laboratories, but it is also anticipated that therapies and biomarkers discovered with high-through-

[\*] Dr. D. M. Vykoukal, Dr. G. P. Stone, Dr. P. R. C. Gascoyne, Dr. E. U. Alt, Dr. J. Vykoukal  
Department of Molecular Pathology, The University of Texas  
M. D. Anderson Cancer Center  
7435 Fannin Street, Houston, TX 77054 (USA)  
Fax: (+1) 713-834-6103  
E-mail: jody@mdanderson.org  
Dr. G. P. Stone  
InGeneron, Incorporated  
8275 El Rio Street, Suite 130, Houston, Texas 77054 (USA)

[\*\*] This research was supported by NIH grant 5R01EB006198 (D.M.V., P.R.C.G., J.V.) and by InGeneron, Inc. (G.P.S.). We thank Caleb Williams, Paul Karazuba, and Joe Camilleri at Aptina Imaging; Robert Riegelsperger at Optical Instrument Laboratory, Inc.; Philip Lorenzi for discussions, and Yasheng Yan for still photography.

Supporting information for this article is available on the WWW under <http://dx.doi.org/10.1002/ange.200901814>.

put techniques will be implemented increasingly at the bedside by using localized assay systems.<sup>[13–15]</sup> The various sample-handling and assay approaches are not disparate or incompatible. The latest-generation flow-injection (FI) methodology of lab-on-valve (LOV) enables assays at the micro- and submicroliter level with low reagent volumes by exploiting miniaturization and integration principles analogous to those that drive the development of lab-on-a-chip devices.<sup>[16,17]</sup> Lab-on-a-chip systems that employ flow injection have also been described.<sup>[18,19]</sup> Furthermore, state-of-the-art high-density microplate instruments are routinely used to manipulate samples with volumes as low as a few microliters; this capacity effectively makes them microfluidic. The current trend for such array-based assay formats is towards higher-density microarray and multiplexed schemes that employ submicroliter sample and reagent volumes.<sup>[20]</sup> Alternatively, 96- and 384-microzone plates fabricated by using paper substrates have recently been described as a low-cost replacement for conventional molded polymer multiwell plates for use in resource-limited laboratories.<sup>[21]</sup> These various approaches are not only compatible, they can also be combined synergistically with microfluidics to yield new means for performing bioassays.<sup>[22]</sup> It is unlikely that any single technology or approach will be suitable for all assays under all circumstances. Rather, systems will emerge from a broad array of available components and demonstrated capabilities, and solutions will be devised that optimize traits such as speed, sensitivity, specificity, ease of use, portability, and cost per assay according to the requirements imposed by and infrastructure of the particular environment in which the technology is to be used.

We sought a compact and cost-effective imaging and detection solution for reagent-droplet tracking and assay quantification for our dielectrophoresis-based microfluidic system. Contact imaging (also referred to as direct or shadow imaging) is achieved by coupling a photodetector array directly to the area to be imaged without intervening optics. Thus, it is ideal for use in microdevices in which the object(s) of interest and the sensor are of a similar scale.<sup>[23–25]</sup>

Efforts in this area have mainly been targeted at providing contact images of particles, cells, and other biological entities. Kovacs and co-workers were the first to demonstrate the use of shadow images from a camera chip attached to the bottom of a microfluidic culture chamber to monitor the activity of *Caenorhabditis elegans* nematodes (typical length, approximately 1 mm) that were maintained in a microfluidic environment.<sup>[23]</sup> Ozcan and co-workers reported a lens-free cell-monitoring technique (LUCAS) for the enumeration of various microparticles by employing image-processing algorithms to recognize signature diffraction patterns (rather than high-resolution images) produced by illuminated polystyrene microbeads, yeast, *Escherichia coli*, erythrocytes, and hepatocytes, for example.<sup>[26]</sup> Yang and co-workers demonstrated a novel lensless contact imager capable of yielding high-resolution images of cells, spores, and nematodes by essentially raster scanning (and then computationally reconstructing) objects that are in translational motion in a micro-channel.<sup>[25]</sup> This optofluidic microscopy (OFM) technique employs an array of custom-fabricated apertures over a 200

pixel linear region to provide intermittent images of 1  $\mu\text{m}$  in diameter spaced 9.9  $\mu\text{m}$  apart. The approach has not been demonstrated for assay detection and may well be of limited utility in this capacity, since the inherent aperture-array mask physically blocks 99.0% of incident photons before they reach the photodetector.

Filippini and Lundström developed a computer-screen-photoassisted technique (CSPT) that employs a computer screen as solid-state light source and a web camera as an optical detector for characterizing and identifying collections of chemical indicators. The approach has been used, for example, to evaluate commercial multiparameter paper-test-strip colorimetric assays<sup>[27]</sup> and to characterize the spectral absorbance and emission responses of porphyrins exposed to various gases and organic vapors in assays on specially prepared thin-film-on-glass sensing arrays.<sup>[28]</sup> Although the CSPT approach does not employ integrated contact imaging and is not explicitly targeted toward microfluidics-based assays, such studies do reveal the feasibility of applying readily available consumer electronic technology to chemical- and biochemical-assay detection. Martinez, Whitesides, and co-workers have described a prototype system for low-cost telemedicine in which paper-based microfluidics and consumer cameras or scanners are used to digitize assays for transmission from remote sites to a central laboratory for analysis by trained evaluators.<sup>[29]</sup>

Herein, we demonstrate that an inexpensive and readily available component can be implemented with channel-, reservoir-, and droplet-based microfluidic architectures and with different standard bioassay chemical reactions to provide quantitative imaging of microscale analyses. To our knowledge, a single, off-the-shelf device that can be applied so ubiquitously for integrated optical detection in labs-on-a-chip has not been described previously.

Our microfluidic device utilizes electrically generated forces to manipulate discrete reagent droplets within an immiscible fluid for the performance of biochemical assays.<sup>[30,31]</sup> A key feature of the system is that reagents are not confined to channels but are instead manipulated freely through the use of an addressable electrode array, which enables the reconfiguration of droplet paths as required for various applications (a number of analogous, *digital* microfluidic approaches are currently being developed).<sup>[32–34]</sup> Since the fluid paths are not predefined, the ability to monitor the position and routing of droplets within the system is useful.

For our application, we chose a commercially available 5 megapixel CMOS image sensor that retails for less than US\$ 20. According to the sensor manufacturer, a complete imaging system can be built from US\$ 40 worth of electronic components by using their reference design and available open-application source code. The use of a mass-produced CMOS sensor provides several advantages. Foremost, since development and production costs are distributed over many millions of unit sales, it is possible to construct an advanced and fully featured component at a reasonable cost per unit. CMOS-fabrication methods enable integration of the photon-sensing array, analog-to-digital signal conversion, image processing, and system control into a single device that outputs quantitative, digital data and requires a minimum of

support components. Furthermore, CMOS fabrication takes advantage of established techniques that are widely used in the volume manufacture of microprocessor and memory devices. The specifications of the image sensor used in these experiments make it suitable for integration with a variety of microfluidic devices other than those we describe herein. The active imaging area is  $5.70 \times 4.28 \text{ mm}^2$  and comprises an array of approximately five million  $2.2 \text{ }\mu\text{m}$  square pixels; it supports both quantitative photodetection and high-resolution contact imaging of typical microfluidic features. The responsivity and low dark current provide low-light-level performance that is acceptable for most applications. Values from neighboring pixels can also be summed to further increase sensitivity or averaged to decrease signal noise as needed. Although such spatial pixel binning results in a concomitant decrease in signal resolution, the use of a high-density array of millions of small light-sensing elements mitigates this effect.

The implementation of our dielectrophoresis-based digital microfluidic device in these studies was based on an array of fluid-handling microelectrodes (Figure 1b) and an upper fluidics layer. The stacked-construction design (Figure 1d) enables the device to be interfaced directly with the imaging surface of the CMOS sensor and attached to the circuit board that carries the sensor and support electronics (Figure 1a,d). This design minimizes the overall system size and is applicable to other microfluidic-device architectures, including those based on glass or polymer microchannels (Figure 2a) or arrays of microfluidic wells or spots (Figure 3a). The design also enables the fabrication of the assay reagents and fluid-handling system in the form of a replaceable cartridge, as opposed to single-use systems, in which assays are performed directly on the sensor itself.<sup>[35]</sup> For our contact-imaging experiments, we utilized a collimated light source (tungsten lamp and modular beam collimator) to minimize diffraction

artifacts and image blurring. The use of a point-source light-emitting diode has also been demonstrated for this purpose.<sup>[23]</sup> The array of  $2.2 \text{ }\mu\text{m}$  pixels enables good imaging of electrode features (Figure 1c), as well as low-resolution imaging of cells and latex microparticles. This straightforward imaging approach also provides visualization and position tracking of nanoliter and smaller reagent droplets (Figure 1e,f; single droplets are shown for clarity). It is therefore practical for general-purpose use in digital microfluidic applications.

As well as in droplet-based schemes, we also evaluated the utility of the CMOS image sensor as a microscale quantitative absorbance detector. We chose a typical microfluidic channel architecture fabricated by using cast polydimethylsiloxane (PDMS) bonded to a glass coverslip. As in the contact-imaging experiments with droplets, the microfluidic assembly was placed directly on the imaging surface of the sensor and transilluminated with collimated light. The lack of intervening optics and large-area ( $24 \text{ mm}^2$ ) sensor array facilitates simple and misalignment-tolerant integration of the microfluidic and detector components. It also enables measurements to be performed on multiple samples in parallel with a single sensor device. The image sensor we chose is produced with integrated RGB Bayer filters that enable multiple-wavelength (600, 530, and 450 nm) absorbance measurements, thus obviating the need for additional optical elements. Also, since the images obtained from the sensor include filtered wavelength data, they are useful for both single and multicolor colorimetric assays (Figure 2a). Such RGB-filter-based optical-detection approaches are also routinely applied in a wide range of conventional microplate-reader systems. An available monochrome version of the CMOS sensor offers better quantum efficiency and would be appropriate for circumstances in which enhanced low-light sensitivity is needed.

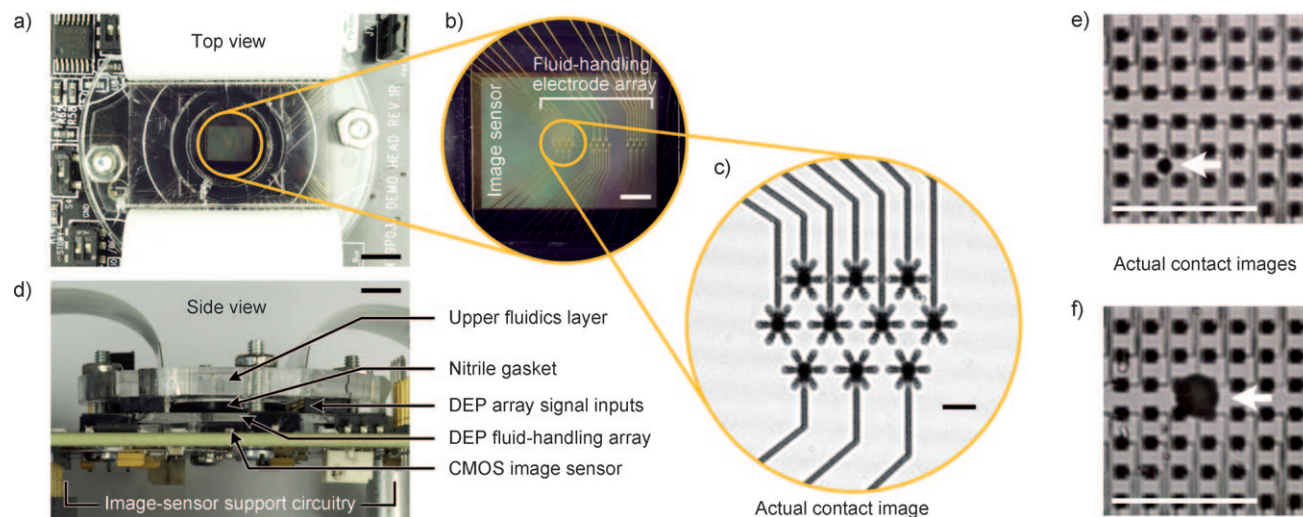


**Figure 1.** CMOS image sensor integrated with a dielectrophoresis-based digital microfluidic device and contact imaging of fluid-handling microelectrodes and reagent droplets. a) Top view of the integrated system comprising a laser-machined polymer fluidics upper layer, a fluid-handling microelectrode array, an image sensor for tracking the position of reagent droplets, and image-sensor support circuitry. b) Magnification of the circled area in (a). Fluid-handling gold microelectrodes positioned over the image sensor. c) Contact image of the circled area in (b) taken with the integrated image sensor. d) Side view of the integrated system showing the stacked construction and compact system size. e,f) Contact images of the microelectrode array and reagent droplets (marked by arrows) obtained with the integrated image sensor. The volumes of the reagent droplets are 0.33 nL (e) and 13.0 nL (f). Scale bars: a,d) 5 mm; b,e,f) 1 mm; c) 125  $\mu\text{m}$ . DEP = dielectrophoresis.



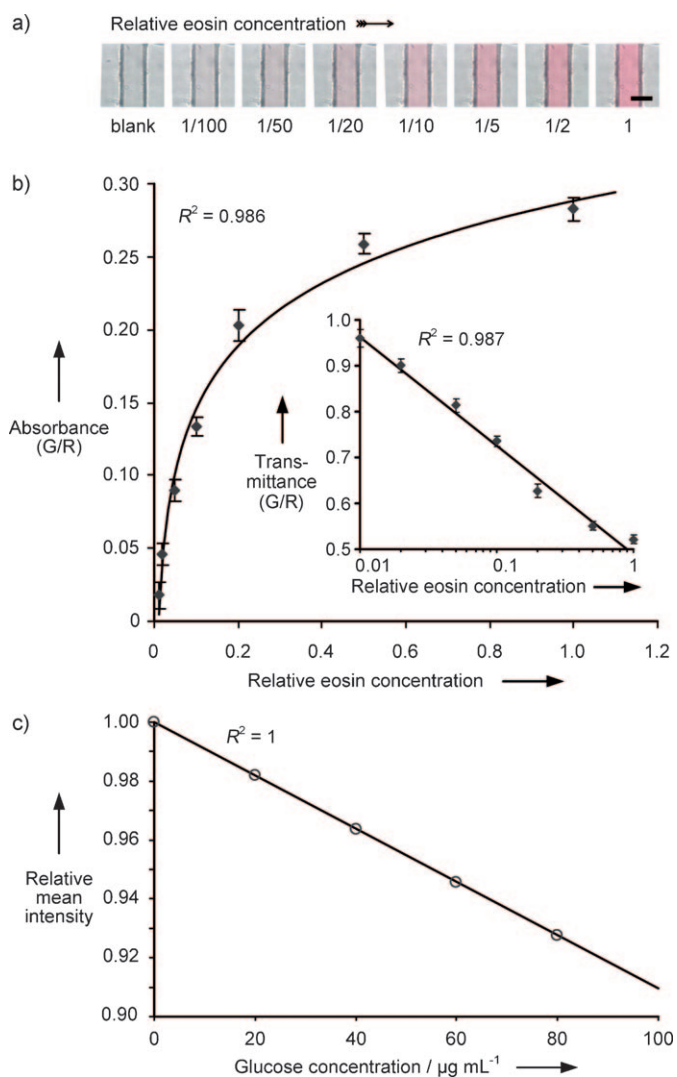


**Figure 2.** Quantitative colorimetric detection and analysis with a commercially available CMOS image sensor. a) Contact images of eosin solutions in a  $200\ \mu\text{m}$  wide  $\times$   $20\ \mu\text{m}$  deep PDMS microchannel. The relative eosin concentration in each solution is noted under its image, with the initial stock designated as “1” and the buffer-only sample designated as “blank”. Scale bar:  $200\ \mu\text{m}$ . b) The absorbance of each of the eosin solutions shown in (a) was determined by analysis of the red (600 nm) and green (530 nm) pixel intensity values as quantified with the image sensor during exposure of the contact image. The inset shows the data as transmittance. c) Colorimetric analysis of glucose concentration by contact imaging. Pixel intensity values were measured with the image sensor to determine the absorbance of oxidized *o*-dianisidine as a function of glucose concentration, as described in the Supporting Information.

For our initial studies, we evaluated solutions of eosin Y, a red dye with its maximum absorption in aqueous solution between 515 and 518 nm. Serial dilutions were prepared from stock to span a range of concentrations across two orders of magnitude. Before analysis of the test solutions, the  $20\ \mu\text{m}$  deep microchannel was filled with water, and the red, green, and blue (RGB) digital gains were adjusted independently to give matched average-intensity values for each color compo-

nent for a multipixel region of interest in the center of the microchannel. Such “white balancing” of the image is akin to zeroing of a conventional spectrophotometer and can be automated readily. Basic image processing was used to find the edges of the channel (they are apparent in the contact image and are distinguished graphically in a plot of the intensity data as regions of low transmittance). The intensity data from the resulting color contact images was analyzed to obtain an absorbance for each sample by comparing the ratio of the pixel intensity at 530 and 600 nm. The mean intensity ratios obtained from a minimum  $1 \times 50$  pixel region of interest in the central area of the channel provided quantitative absorbance data that correlated well with eosin Y concentration over a 100-fold concentration range (Figure 2b). Through the averaging of data from several neighboring photodetectors, the signal-to-noise ratio of the absorbance measurements is increased, as evidenced by the small relative error and good fit of the trend lines.

To demonstrate that the sensor can be applied to biochemical analyses based on chemical reactions with commonly used reagents, we also performed a colorimetric glucose assay. Specifically, we chose a standard coupled enzyme assay in which the conversion of glucose into gluconic acid is linked proportionally to the oxidation of *o*-dianisidine to form a colored product, the absorbance of which is measured at 540 nm. The samples were again contained within a microfluidic layer placed directly on top of the sensor. We were able to quantitatively image glucose solution concentrations that spanned the recommended working range of the assay. A plot of the relative averaged green-pixel intensity versus glucose concentration generated a linear standard curve with excellent trend-line-fit statistics (Figure 2c). The results are similar to those that would be expected from a conventional spectrophotometer.

Although absorbance-based methods are employed routinely in bioanalysis, they can be difficult to apply to the analysis of highly colored matrices, such as whole blood. For such analyses, methods based on fluorescence or luminescence would be preferred. Also, sensitive colorimetric determination can be problematic to implement in microfluidics because of the inherently short optical path lengths. Whitesides and co-workers developed a low-cost single-channel optical sensor and alternative immunoassay chemistry based on the reduction of silver ions to an opaque silver film to circumvent this problem.<sup>[36]</sup> Assay methods that function on the basis of chemiluminescent reactions which produce their own light<sup>[37]</sup> are widely available and can also be used to overcome this difficulty. Furthermore, the use of assays based on such reactions simplifies system integration by eliminating the need for an excitation source. We investigated the applicability of the CMOS image sensor as a microscale photometer for the quantitative detection of chemiluminescent reactions, again by employing a contact-imaging approach. Accordingly, we incubated a bioluminescent reagent intended for the screening of kinase activity (Kinase Glo Plus, Promega Corporation) with its substrate, adenosine-5'-triphosphate (ATP), in various concentrations. The reactions were contained in an array of microwells of 1 mm in diameter (comparable to the diameter of individual wells on a

1536 well microplate) that was fabricated on a glass coverslip and placed directly on the sensor imaging surface. A repurposed black phenolic bottle cap was used to protect the array assembly from stray light, and the array chemiluminescence was integrated by using a 200 ms exposure. The resulting contact image of the array (Figure 3a) reveals the

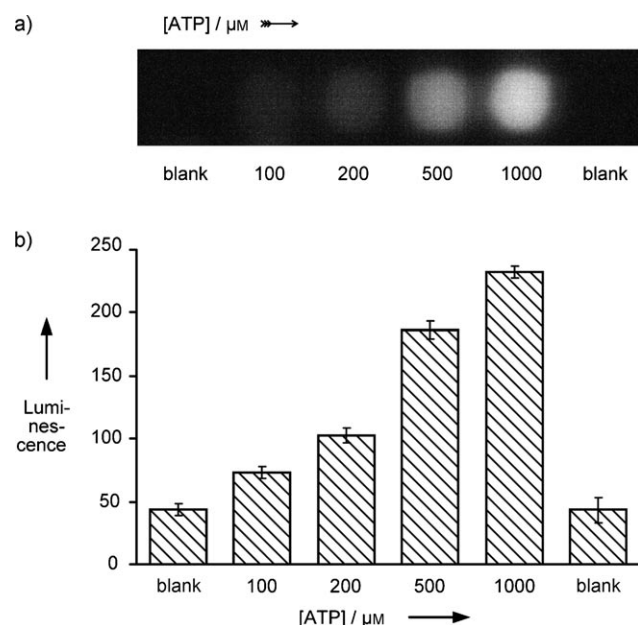


**Figure 3.** Quantitative bioluminescent detection and analysis with a commercially available CMOS image sensor. a) Contact images of Kinase Glo Plus assay reactions in an array of polymer microwells of 1 mm in diameter. The ATP concentration in each reaction mixture is noted under the corresponding image; the controls without ATP are designated as “blank”. b) The relative chemiluminescence (in arbitrary units) of each reaction mixture shown in (a) was determined by analysis of the blue (450 nm) pixel intensity values as quantified with the image sensor during exposure of the contact image (see the Supporting Information for details).

different ATP concentration in each well across a 10-fold concentration range. The relative chemiluminescence of each sample was quantified (Figure 3b) by averaging the intensity data from a  $1 \times 100$  pixel region of interest (approximately 20% of the diameter) from the center of each microwell. As in the absorbance studies, the averaging of data from multiple pixels increased the signal-to-noise ratio, and a good correlation between the measured intensity and reagent concentration was observed.

Indeed, for applications in which analytes need to be analyzed rapidly or at exceedingly low concentrations, the ultimate detection sensitivity of the analysis platform is the foremost parameter of concern. Assay systems in which photomultiplier tubes, avalanche photodiodes, and (more recently) low-noise, cooled-CCD cameras (CCD = charge-coupled device) are used have impressive gain and dynamic-range properties, and are capable of limits of detection down to at least picomolar sensitivity.<sup>[7]</sup> Such performance is not, however, inexpensive, as plate readers or other analysis

platforms that employ these high-performance detectors are generally priced in the US\$ 10 000–100 000 range. Similar to the manner in which CCD image sensors are implemented for purposes that were once the exclusive domain of more costly detectors, advances in detector technology are narrowing the performance gap between CMOS- and CCD-based image sensors. Furthermore, detection limits for a given assay system are a function of both the detector and the reporter chemistry used, and signal amplification is possible through both of these system components. The use of a less sensitive detector may necessitate an appropriately compensatory assay approach based on alternative or novel reporter schemes to amplify analyte signals to a suitable level.

In summary, these investigations demonstrate that it is possible to use a low-cost and readily available CMOS sensor chip as a microscale contact imager for droplet-based microfluidics and as a quantitative photometer for the integrated optical detection of typical absorbance and chemiluminescence assays implemented on a microfluidic platform. We anticipate that the utility of the method can be expanded by incorporating a capacity for fluorescence-based assays. The use of contact imaging for lab-on-a-chip detection simplifies system integration, eliminates the need for the precision alignment of multiple optical components, and is applicable to the most common microfluidic architectures, including those based on channels, reservoirs, and droplets. In applications in which the overall cost of the assay system is the factor that must be optimized, readily available CMOS image sensors provide an assay-detection solution with an exceptional price-to-performance ratio. Their use in this capacity certainly merits further exploration.

### Experimental Section

Contact imaging was performed with an Aptina MT9P031I12STC image sensor. The fluid-handling microelectrodes were fabricated by standard microlithographic processing of thin-film substrates, and the fluidics layer was fabricated from sheet acrylic. Droplet manipulation by dielectrophoresis is described in detail elsewhere.<sup>[30,31]</sup> For the colorimetric assays, microchannels were cast in PDMS elastomer by using a negative mold and bonded to a glass coverslip. Eosin was diluted in deionized water. Each data point is the average value from a region containing more than 50 pixels in the channel center. For the glucose assays, the Sigma–Aldrich glucose oxidase assay kit GAGO-20 was used according to the protocol provided by the manufacturer. Reaction mixtures were loaded into hybriwells affixed to glass coverslips and contact imaged. Each data point is the mean intensity value for a 2025 pixel region. For the bioluminescence assays, a microwell array was constructed from a polyester sheet and a glass coverslip. Promega Kinase-Glo Plus Luminescent Kinase Assay was used according to the protocol provided by the manufacturer. ATP was diluted into kinase buffer. Chemiluminescent reaction mixtures were loaded into microwells and contact imaged. Each data point is the average from a 100 pixel region in the center of each well. See the Supporting Information for further experimental details.

Received: April 3, 2009

Revised: July 29, 2009

Published online: September 4, 2009

**Keywords:** analytical methods · colorimetry · droplets · luminescence · microfluidics

- [1] B. Hay, J. Wasserman, C. A. Dahl, *Nature* **2006**, *SI*, 1–2.
- [2] M. Urdea, L. A. Penny, S. S. Olmsted, M. Y. Giovanni, P. Kaspar, A. Shepherd, P. Wilson, C. A. Dahl, S. Buchsbaum, G. Moeller, B. Hay, *Nature* **2006**, *444*, 73–79.
- [3] P. Yager, G. J. Domingo, J. Gerdes, *Annu. Rev. Biomed. Eng.* **2008**, *10*, 107–144.
- [4] F. B. Myers, L. P. Lee, *Lab Chip* **2008**, *8*, 2015–2031.
- [5] G. M. Whitesides, *Nature* **2006**, *442*, 368–373.
- [6] J. West, M. Becker, S. Tombrink, A. Manz, *Anal. Chem.* **2008**, *80*, 4403–4419.
- [7] D. Brennan, J. Justice, B. Corbett, T. McCarthy, P. Galvin, *Anal. Bioanal. Chem.* **2009**, DOI: 10.1007/s00216-009-2826-5.
- [8] G. J. Kost, N. K. Tran, M. Tuntideelert, S. Kulrattanamaneepon, N. Peungposop, *Am. J. Clin. Pathol.* **2006**, *126*, 513–520.
- [9] J. Ruzicka, E. H. Hansen, *Anal. Chem.* **2000**, *72*, 212A–217A.
- [10] J. Ruzicka, E. H. Hansen, *TrAC-Trends Anal. Chem.* **2008**, *27*, 390–393.
- [11] T. Chapman, *Nature* **2003**, *421*, 661–666.
- [12] N. Blow, *Nat. Methods* **2008**, *5*, 109–112.
- [13] J. Kling, *Nat. Biotechnol.* **2006**, *24*, 891–893.
- [14] P. K. Sorger, *Nat. Biotechnol.* **2008**, *26*, 1345–1346.
- [15] R. Mukhopadhyay, *Anal. Chem.* **2009**, *81*, 4169–4173.
- [16] J. Ruzicka, *Analyst* **2000**, *125*, 1053–1060.
- [17] X. W. Chen, J. H. Wang, *Anal. Chim. Acta* **2007**, *602*, 173–180.
- [18] Z. R. Xu, C. H. Zhong, Y. X. Guan, X. W. Chen, J. H. Wang, Z. L. Fang, *Lab Chip* **2008**, *8*, 1658–1663.
- [19] B. E. Rapp, L. Carneiro, K. Lange, M. Rapp, *Lab Chip* **2009**, *9*, 354–356.
- [20] M. M. Ling, C. Ricks, P. Lea, *Expert Rev. Mol. Diagn.* **2007**, *7*, 87–98.
- [21] E. Carrilho, S. T. Phillips, S. J. Vella, A. W. Martinez, G. M. Whitesides, *Anal. Chem.* **2009**, DOI: 10.1021/ac900847g.
- [22] S. Derveaux, B. G. Stubbe, K. Braeckmans, C. Roelant, K. Sato, J. Demeester, S. C. De Smedt, *Anal. Bioanal. Chem.* **2008**, *391*, 2453–2467.
- [23] D. Lange, C. W. Storment, C. A. Conley, G. T. A. Kovacs, *Sens. Actuators B* **2005**, *107*, 904–914.
- [24] H. H. Ji, D. Sander, A. Haas, P. A. Abshire, *IEEE Trans. Circuits Syst. I* **2007**, *54*, 1698–1710.
- [25] X. Cui, L. M. Lee, X. Heng, W. Zhong, P. W. Sternberg, D. Psaltis, C. Yang, *Proc. Natl. Acad. Sci. USA* **2008**, *105*, 10670–10675.
- [26] S. Seo, T. W. Su, D. K. Tseng, A. Erlinger, A. Ozcan, *Lab Chip* **2009**, *9*, 777–787.
- [27] D. Filippini, I. Lundström, *Analyst* **2006**, *131*, 111–117.
- [28] D. Filippini, A. Alimelli, N. C. Di, R. Paolesse, A. D'Amico, I. Lundström, *Angew. Chem.* **2006**, *118*, 3884–3887; *Angew. Chem. Int. Ed.* **2006**, *45*, 3800–3803.
- [29] A. W. Martinez, S. T. Phillips, E. Carrilho, S. W. Thomas III, H. Sindi, G. M. Whitesides, *Anal. Chem.* **2008**, *80*, 3699–3707.
- [30] J. A. Schwartz, J. V. Vykoukal, P. R. Gascoyne, *Lab Chip* **2004**, *4*, 11–17.
- [31] P. R. Gascoyne, J. V. Vykoukal, J. A. Schwartz, T. J. Anderson, D. M. Vykoukal, K. W. Current, C. McConaghy, F. F. Becker, C. Andrews, *Lab Chip* **2004**, *4*, 299–309.
- [32] S. Y. Teh, R. Lin, L. H. Hung, A. P. Lee, *Lab Chip* **2008**, *8*, 198–220.
- [33] R. Sista, Z. Hua, P. Thwar, A. Sudarsan, V. Srinivasan, A. Eckhardt, M. Pollack, V. Pamula, *Lab Chip* **2008**, *8*, 2091–2104.
- [34] J. Gong, C. J. Kim, *Lab Chip* **2008**, *8*, 898–906.
- [35] F. Mallard, G. Marchand, F. Ginot, R. Campagnolo, *Biosens. Bioelectron.* **2005**, *20*, 1813–1820.
- [36] S. K. Sia, V. Linder, B. A. Parviz, A. Siegel, G. M. Whitesides, *Angew. Chem.* **2004**, *116*, 504–508; *Angew. Chem. Int. Ed.* **2004**, *43*, 498–502.
- [37] B. Filanoski, S. K. Rastogi, E. Cameron, N. N. Mishra, W. Maki, G. Maki, *Luminescence* **2008**, *23*, 22–27.